

NUMERICAL SIMULATION OF COMPRESSIBLE FLOW THROUGH CASCADE OF PROFILES

VÍT DOLEJŠÍ

*Department of Numerical Mathematics,
Charles University Prague,
Sokolovska 83, 18600 Praha 8, Czech Republic
dolejsi@karlin.mff.cuni.cz*

(Received 20 July 2001; revised manuscript received 10 October 2001)

Abstract: We deal with the numerical simulation of flow through a steam turbine. The system of the compressible Navier-Stokes equations accompanied by the state equation of perfect gas are numerically solved. We propose a new approach for the numerical solution of the Navier-Stokes equations, where the inviscid part is discretized by the finite volume method and the viscous part by the finite element method. To capture precisely the position of shock waves, the suitable mesh refinement method has to be applied. Therefore the anisotropic mesh adaptation technique equipped with some suitable modification for viscous compressible flow is used. The suitable application of the mentioned numerical adaptive method allows us to obtain sufficiently precise results without much requirement on CPU-time and computer memory.

Keywords: compressible Navier-Stokes equations, combined finite volume-finite element method, anisotropic mesh adaptation

1. Introduction

The results of aerodynamic research tests of profile cascades at transonic flow velocities are invaluable for improvements of new machine designs and verification on the routine test methods. Higher efficiency and operational reliability of new turbines and compressors are attainable largely due to such experimental research programs.

Our aim is a numerical simulation of transonic flow past a plane turbine cascade SE 1050 (ŠKODA – Etalon 1050) which approximates the flow through a steam turbine. The rotational symmetry of the turbine allows the 2D computation (see [1, 2]). Then the region occupied by the fluid is represented by a plane infinitely connected domain $\tilde{\Omega}$, bounded in one space direction (say x_1) and unbounded but periodic in the other direction (x_2). Assuming also the periodicity of the flow field, we can choose the computational domain Ω in the form of one period of the original domain $\tilde{\Omega}$, Figure 1. The boundary $\partial\Omega$ is formed by disjoint parts $\Gamma_I, \Gamma_O, \Gamma_W, \Gamma^+$ and Γ^- . The parts Γ_I and Γ_O denote inlet and outlet of the computational domain Ω ,

respectively, and Γ_W denotes solid walls of a blade of the cascade. Moreover, the arcs Γ^- and Γ^+ are piecewise linear artificial cuts such that

$$\Gamma^+ = \{(x_1, x_2 + q); (x_1, x_2) \in \Gamma^-\}, \quad (1)$$

where $q > 0$ is the width of one period of the cascade in the direction x_2 .

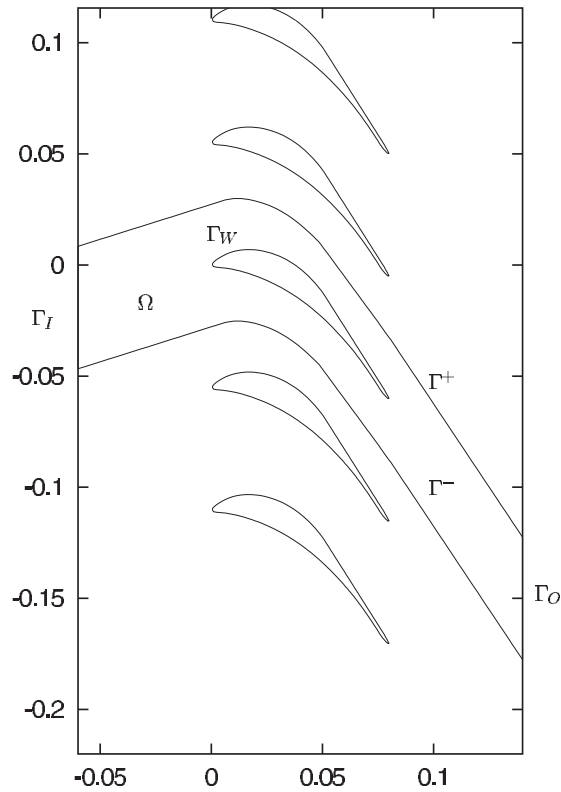


Figure 1. Cascade SE 1050 with the computational domain Ω , boundary parts Γ_I , Γ_O , Γ_W and artificial periodical cuts Γ^+ and Γ^-

2. Problem formulation

The behaviour of a gas in the steam turbine is described by basic conservation laws: conservation of mass, momentum and energy. We consider a viscous compressible fluid of Newtonian type, *i.e.* the dependence of stress tensor on the deformation velocity tensor is linear. We neglect outer volume forces and heat sources. The heat conduction is given by the Fourier law. To close the system of equations we add the state equation of perfect gas.

Therefore, the complete system for viscous compressible flow consisting of the continuity equation, Navier-Stokes equations and energy equation is written in the (dimensionless) form

$$\frac{\partial w}{\partial t} + \sum_{s=1}^2 \frac{\partial f_s(w)}{\partial x_s} = \sum_{s=1}^2 \frac{\partial R_s(w, \nabla w)}{\partial x_s} \quad \text{in } Q_T. \quad (2)$$

This form is obtained by dividing the original conservation laws by the reference flow parameters, see [3]. Here

$$\begin{aligned}
 w &= (w_1, w_2, w_3, w_4)^T = (\rho, \rho v_1, \rho v_2, e)^T, \\
 w &= w(x, t), \quad x \in \Omega, \quad t \in (0, T), \\
 f_s(w) &= (\rho v_s, \rho v_s v_1 + \delta_{s1} p, \rho v_s v_2 + \delta_{s2} p, (e + p) v_s)^T, \\
 R_s(w, \nabla w) &= \left(0, \tau_{s1}, \tau_{s2}, \tau_{s1} v_1 + \tau_{s2} v_2 + \frac{\gamma}{\text{RePr}} \frac{\partial \theta}{\partial x_i} \right)^T, \\
 \tau_{sr} &= \frac{1}{\text{Re}} \left[\left(\frac{\partial v_s}{\partial x_r} + \frac{\partial v_r}{\partial x_s} \right) - \frac{2}{3} \text{div} \mathbf{v} \delta_{sr} \right], \quad s, r = 1, 2.
 \end{aligned} \tag{3}$$

From thermodynamics we have

$$p = (\gamma - 1)(e - \rho |\mathbf{v}|^2 / 2), \quad e = \rho(\theta + |\mathbf{v}|^2 / 2). \tag{4}$$

We use the standard notation for dimensionless quantities: t is time, x_1, x_2 are Cartesian coordinates in \mathbb{R}^2 , ρ is density, $\mathbf{v} = (v_1, v_2)$ is velocity vector with components v_s in the directions x_s , $s = 1, 2$, p is pressure, θ is temperature, e is total energy, τ_{sr} are components of the viscous part of the stress tensor, δ_{sr} is Kronecker delta, $\gamma > 1$ is Poisson adiabatic constant, Re is Reynolds number, Pr is Prandtl number. Moreover, we define $M = |\mathbf{v}| / (\gamma p / \rho)^{1/2}$ for the local Mach number.

The system (2) – (4) is equipped with the initial condition

$$w(x, 0) = w^0(x), \quad x \in \Omega \tag{5}$$

(which means that at time $t = 0$ we prescribe, *e.g.* ρ, v_1, v_2 and θ) and boundary conditions.

The correct setting of the boundary conditions for the system (2) is still an open problem because, from the mathematical point of view, there is nothing known about the existence and uniqueness of its solution. So based on several heuristic consideration (see [3, 4]) and vast numerical experience, we prescribe the following boundary conditions:

$$\begin{aligned}
 \text{(i)} \quad & \rho = \rho^*, \quad v_s = v_s^*, \quad s = 1, 2, \quad \frac{\partial \theta}{\partial n} = 0 \quad \text{on } \Gamma_I, \\
 \text{(ii)} \quad & v_s = 0, \quad s = 1, 2, \quad \frac{\partial \theta}{\partial n} = 0 \quad \text{on } \Gamma_W, \\
 \text{(iii)} \quad & \sum_{s=1}^2 \tau_{sr} n_s = 0, \quad r = 1, 2, \quad \frac{\partial \theta}{\partial n} = 0 \quad \text{on } \Gamma_O.
 \end{aligned} \tag{6}$$

Here $\partial/\partial n$ denotes the derivative in the direction of the unit outer normal $\mathbf{n} = (n_1, n_2)^T$ to $\partial\Omega$; w^0, ρ^* and v_s^* are given functions.

On Γ^\pm we consider the periodicity condition

$$w(x_1, x_2 + q, t) = w(x_1, x_2, t), \quad (x_1, x_2) \in \Gamma^-. \tag{7}$$

The same condition is imposed on the first-order derivatives of the vector function w .

3. Discretisation

We consider the viscous terms R_s as a perturbation of the inviscid system of Euler equations. Therefore, we split Equation (2) into the inviscid system and the purely viscous system

$$\frac{\partial w}{\partial t} + \sum_{s=1}^2 \frac{\partial f_s(w)}{\partial x_s} = 0, \quad (8)$$

$$\frac{\partial w}{\partial t} = \sum_{s=1}^2 \frac{\partial R_s(w, \nabla w)}{\partial x_s} \quad (9)$$

and discretize them separately.

The time discretisation of Equations (8) and (9) is carried out with the use of a partition $0 = t_0 < t_1 < t_2 < \dots$ of the time interval $(0, T)$. We set $\tau_k = t_{k+1} - t_k$.

The inviscid system (8) is discretized by the cell-centred *finite volume (FV) method* on a mesh $\mathcal{D}_h = \{D_i\}_{i \in J}$. Here the finite volumes D_i are triangles and \mathcal{D}_h is a triangulation of a polygonal approximation Ω_h of the domain Ω . We assume that \mathcal{D}_h has standard properties from the finite element method. J is a suitable index set. The boundary ∂D_i can be expressed in the form

$$\partial D_i = \bigcup_{j \in S(i)} \Gamma_{ij}, \quad (10)$$

where Γ_{ij} is either the common side of D_i and D_j or $\Gamma_{ij} \subset \partial \Omega_h$. We set $|D_i| = \text{area of } D_i$, $\mathbf{n}_{ij} = \text{unit outer normal to } \partial D_i \text{ on } \Gamma_{ij}$, $\ell_{ij} = \text{length of } \Gamma_{ij}$. $S(i)$ is a suitable index set. The averages of the sought solution w on D_i at time t_k are approximated by values w_i^k .

The *purely viscous system* (9) is discretized by the conforming piecewise linear *finite elements (FE)* on a triangulation \mathcal{T}_h of Ω_h , compatible with \mathcal{D}_h in such a sense that the set of all vertices P_i of the triangles $T \in \mathcal{T}_h$ consists of the barycentres of all $D_i \in \mathcal{D}_h$ and the vertices of $D_i \in \mathcal{D}_h$ lying on $\partial \Omega_h$. We call this mesh \mathcal{T}_h *adjoint* to the grid \mathcal{D}_h .

Using the above ideas, we discretize the complete system (1) via *operator inviscid-viscous splitting*. The advantage of this approach is that we easily evaluate both the values of the physical quantities (on mesh \mathcal{D}_h) and their derivatives (on mesh \mathcal{T}_h). Moreover, the hyperbolic and parabolic types of the systems (8) and (9) give a hint to use FVM and FEM, respectively.

One time step $t_k \rightarrow t_{k+1}$ is divided into two *fractional steps*:

Step I (*inviscid FV step on the mesh \mathcal{D}_h*): Assume that the values w_i^k , $i \in J$, approximating the solution on the finite volumes D_i at time t_k are known. Compute the values $w_i^{k+1/2}$, $i \in J$, from the FV formula

$$w_i^{k+1/2} = w_i^k - \frac{\tau_k}{|D_i|} \sum_{j \in S(i)} H(w_i^k, w_j^k, \mathbf{n}_{ij}) \ell_{ij} \quad (11)$$

equipped with inviscid boundary conditions.

Step II (*viscous FE step on the mesh \mathcal{T}_h*): Define the finite element function $w_h^{k+1/2}$ with values $w_h^{k+1/2}(P_i) = w_i^{k+1/2}$ at the vertices P_i , $i \in J$ of \mathcal{T}_h . At the vertices $P_i \in \partial \Omega_h$, the viscous Dirichlet boundary conditions and suitable

extrapolation are used. Compute the finite element function w_h^{k+1} as the solution of the following problem:

- (i) w_h^{k+1} satisfies the viscous Dirichlet boundary conditions,
- (ii) $(w_h^{k+1}, \varphi_h)_h = (w_h^{k+1/2}, \varphi_h)_h - \tau_k a_h(w_h^{k+1/2}, \varphi_h)$ (12)
 for all test functions $\varphi_h = (\phi_1, \dots, \phi_4)$ such that ϕ_j ($j = 1, \dots, 4$) is continuous in Ω_h , linear on each $T \in \mathcal{T}_h$ and vanishes on the part of $\partial\Omega_h$ where the j -th component w_j of the state vector w satisfies the Dirichlet boundary condition.

Now set $w_i^{k+1} := w_h^{k+1}(P_i)$ for $i \in J$, $k := k + 1$ and go to Step I.

In Equation (11), H is a suitable numerical flux. We use the Osher-Solomon numerical flux [5] which is an upwinding type of scheme not requiring any other artificial viscosity term. Moreover the Osher-Solomon numerical flux contains some amount of numerical viscosity which guarantees that we obtain the physically admissible numerical solution (*i.e.* satisfying the second law of thermodynamic).

In Equation (12), $(w, \varphi)_h$ and $a_h(w, \varphi)$ denote the approximation of $\int_{\Omega_h} w \varphi dx$ and $\int_{\Omega_h} \sum_{s=1}^2 R_s(w, \nabla w) \partial \varphi / \partial x_s dx$, respectively, obtained with the aid of numerical quadrature using the vertices of $T \in \mathcal{T}_h$ as integration points. For more detail see [4, 6]. Another approach can be found in [7].

The presented scheme is only of the first order or accuracy. To increase it (at least to the second order) we apply the higher order reconstruction [8]. Further work is in progress.

The accuracy of the solution of transonic flow is increased with the aid of the automatic adaptive mesh refinement, namely in the vicinity of shock waves and boundary layers.

4. Mesh adaptivity

To improve the quality of a solution *the anisotropic mesh adaptation* (AMA) technique is applied. We adapt the triangulation in this way that *the interpolation error* (defined as the distance between the exact solution and its piecewise linear approximation) is uniformly distributed over the whole triangulation. The complete description of the AMA technique with some theoretical results and the algorithm with implementation was given in [9–11]. Here we present only a brief description.

Let M be a symmetric positive definite 2×2 matrix and let $\mathbf{u} = (u_1, u_2)$ be a vector in \mathbb{R}^2 . We define *the norm* of the vector \mathbf{u} corresponding to the matrix M as

$$\|\mathbf{u}\|_M \equiv (\mathbf{u} M \mathbf{u}^T)^{\frac{1}{2}}. \tag{13}$$

Let \mathcal{T} be a triangulation of the computational domain Ω_h . Let M_k be a symmetric positive definite 2×2 matrix defined for each edge of the triangulation S_k , $k \in K$ (= an index set) by

$$M_k = F(\mathbf{H}(\eta(S_k))), \quad k \in K, \tag{14}$$

where η is some physical quantity (we put $\eta :=$ Mach number), \mathbf{H} is the Hessian matrix of η and $F: \mathcal{M}^2 \rightarrow \mathcal{M}^2$ is a suitable function, \mathcal{M}^2 is the space of 2×2 matrixes.

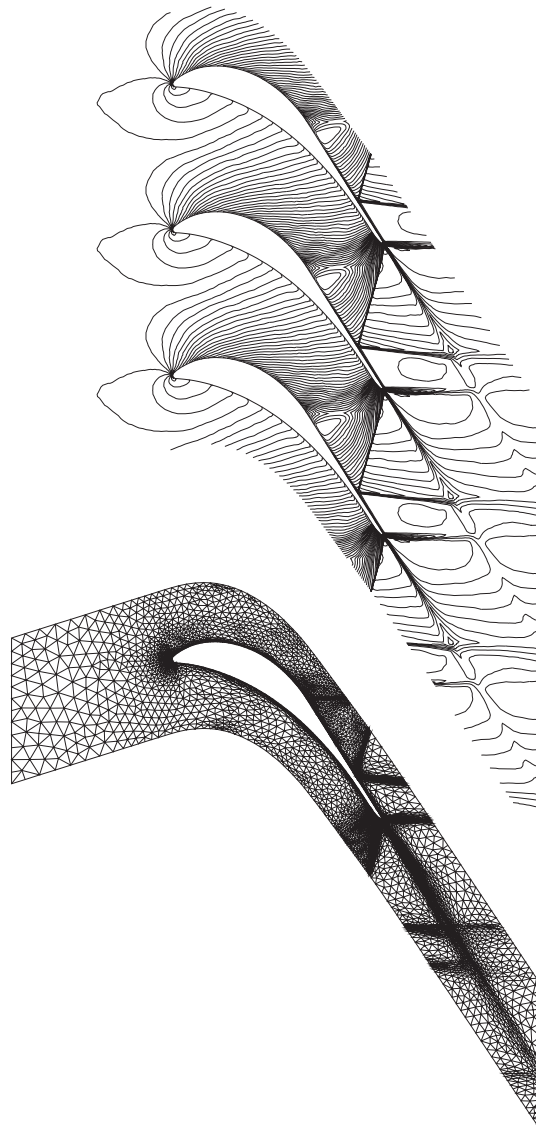


Figure 2. Density isolines (top) and the final triangular mesh (bottom)

The form of the function F follows from some heuristic considerations and numerical experiments, see [11].

Now, we say that the mesh \mathcal{T} is *optimal* if the norm of S_k corresponding to \bar{M}_k is equal to $\sqrt{3}$ for all $k \in K$, *i. e.*

$$\|S_k\|_{M_k} = \sqrt{3} \quad \forall k \in K. \quad (15)$$

It means that the error (considered as $\|\cdot\|_M$) for each edge of \mathcal{T} is the same, *i. e.* it is uniformly distributed over the triangulation. If $M_k = I$ (= a unit matrix) for all $k \in K$, then the optimal triangulation consists of equilateral triangles with the length of sides equal to $\sqrt{3}$. (The radius of the circles circumscribing this triangles is equal

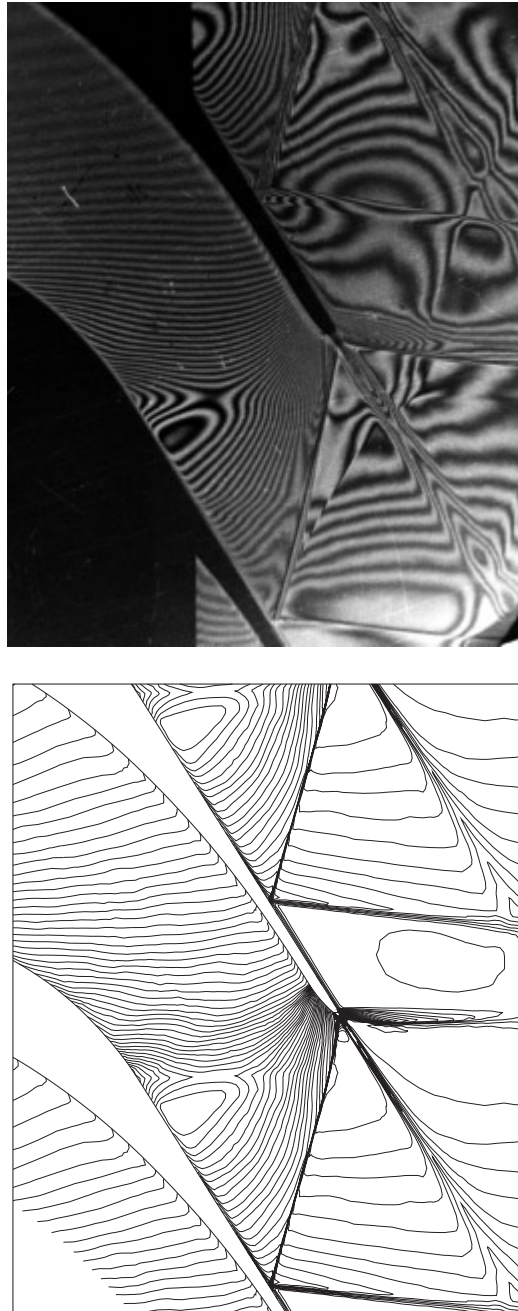


Figure 3. The wind tunnel interferogram showing density isolines (top) and the corresponding detail of density isolines (bottom)

to 1, this is the reason why a scaling constant $\sqrt{3}$ is chosen.) We define *the quality parameter*

$$Q_T = \frac{1}{N_T} \sum_{k \in K} \left(\|S_k\|_{M_k} - \sqrt{3} \right)^2, \quad (16)$$

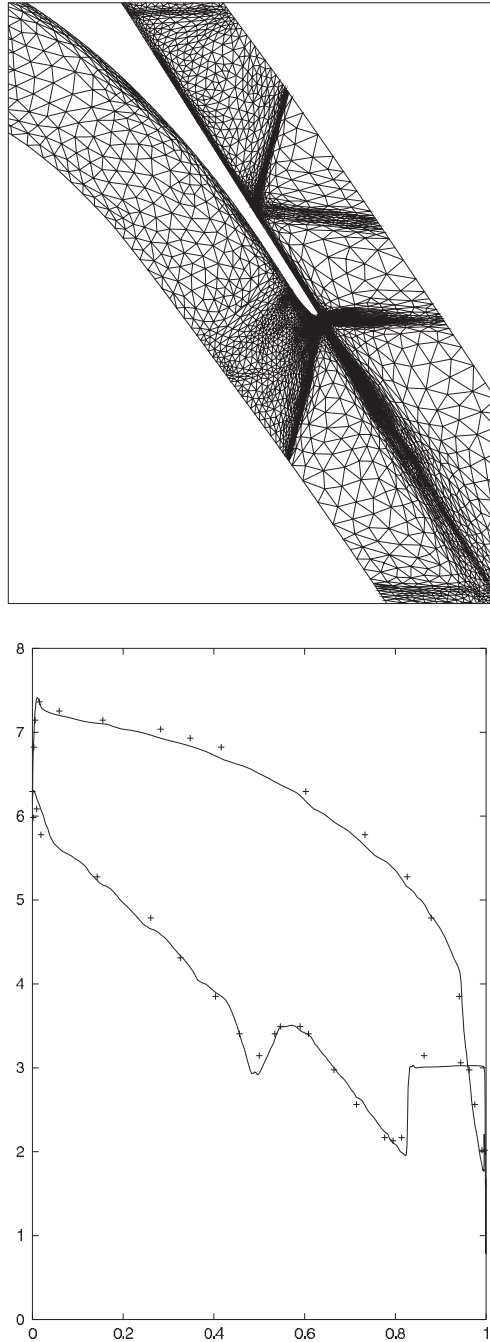


Figure 4. Detail of final triangulation (top) and pressure distribution along the profile “full line” compared with the measurement “separated crosses” (bottom)

where $\|S_k\|_{M_k}$ is the norm of the edge S_k and $N_{\mathcal{T}}$ is the number of all edges of \mathcal{T} . It is evident that $Q_{\mathcal{T}} \geq 0$ and if the mesh \mathcal{T} is optimal then $Q_{\mathcal{T}} = 0$. The parameter $Q_{\mathcal{T}}$ is a measure how close the triangulation \mathcal{T} is to the optimal one. We modify the mesh \mathcal{T} in this way that the quality parameter is minimized. Therefore we have developed an

iterative process which is a composition of the local operations: adding a node at the center of an edge, removing an edge, swapping the diagonal of the quadrilateral formed by any pair of adjacent elements, and moving a node. Each operation is performed if after its application the parameter $Q_{\mathcal{T}}$ decreases.

Special attention is devoted for capturing viscous effects of a flow, namely boundary layers and wakes. As the boundary layer thickness δ is given by

$$\delta \approx \frac{C}{\sqrt{\text{Re}}}, \quad (17)$$

where Re is the Reynolds number and $C \gg 1$ is a “user-chosen” constant (we put $C = 10$), we modify the mentioned AMA algorithm in such a way that the size of triangles in the vicinity of Γ_W is less than δ , see [10].

The multiple application of AMA algorithm yields the triangulation with a not too large number of triangles but where satisfactory results can be obtained.

5. Numerical results

The goal was to obtain a steady state solution with the aid of the time stabilisation for $t \rightarrow \infty$. The computational results are compared with a wind tunnel experiment (by courtesy of the Institute of Thermomechanics of the Czech Academy of Sciences in Prague, see [1]). The experiment and computations were performed for the following data: angle of attack = $19^\circ 18'$, inlet Mach number = 0.32, outlet Mach number = 1.18, $\gamma = 1.4$, Reynolds number $\text{Re} = 1.5 \cdot 10^6$, Prandtl number $\text{Pr} = 0.72$.

In Figure 2, the final triangular mesh obtained with the aid of AMA and the computed density isolines are plotted. Figure 3 represents the comparison of the wind tunnel interferogram showing density isolines with detail of our results. Figure 4 shows the detail of the final triangular mesh and the pressure distribution along the profile compared with the measurement. We see a good agreement of the computational results with experiment, namely the position of shock waves and the rarefaction region. Particularly, the use of AMA enable us to capture shock waves very sharply without much increase of the number of elements. Moreover the quantitative comparison of the pressure distribution is very satisfactory. Our mathematical model does not contain any model of turbulence. The results confirm the fact that the turbulence effects for the considered problem are not leading even for $\text{Re} = 1.5 \cdot 10^6$.

6. Conclusion

The presented finite volume – finite element scheme together with the anisotropic mesh adaptation introduce the efficient numerical method for the simulation of transonic flow problems which is confirmed by the achieved numerical results. The future work is to develop the higher order schemes in order to increase the accuracy of the results and to eliminate the influence of numerical viscosity.

Acknowledgements

This research has been supported under Grant No. 275/20B MAT/MFF and Grant No. MSM 113200007.

References

- [1] Štastný M and Šafařík P 1990 *ASME Paper 90-GT-313*

- [2] Štastný M and Šafařík P 1992 *ASME Paper* **92-GT-155**
- [3] Feistauer M 1993 *Mathematical Methods in Fluid Dynamics*, Longman Scientific & Technical, Harlow
- [4] Feistauer M and Felcman J 1996 *The Mathematics of Finite Elements and Applications*, ed. Whitemen J R, John Wiley & Sons, pp. 175–194
- [5] Osher S and Solomon F 1982 *Math. Comp.* **38** 339
- [6] Feistauer M, Felcman J and Lukáčová M 1995 *J. Comput. Appl. Math.* **63** 179
- [7] Fort J, Furst J, Halama J and Kozel K 2000 *ZAMM* **80** (3) 607
- [8] Felcman J and Dolejší V 1998 *J. Engineering Mechanics* **5** 327
- [9] Dolejší V 1998 *Computing and Visualisation in Science* **1** (3) 165
- [10] Dolejší V 2001 *East-West J. Numerical Mathematics* **9** (1) 1
- [11] Dolejší V and Felcman J 2000, submitted to *Numerical Methods for Partial Differential Equations*